Analysis of the Interactions of Actin Depolymerizing Factor with G- and F-Actin†

S. M. Hayden,‡ P. S. Miller, A. Brauweiler, and J. R. Bamburg*

Department of Biochemistry, Program in Neuronal Growth and Development, and Graduate Program of Cellular and Molecular Biology, Colorado State University, Fort Collins, Colorado 80523

Received April 26, 1993; Revised Manuscript Received July 2, 1993•

ABSTRACT: Chick actin depolymerizing factor (ADF) is an actin binding protein previously shown to rapidly depolymerize actin filaments *in vitro*, yielding a 1:1 complex of ADF and actin monomer. Here we show that ADF protects actin monomer from denaturation by EDTA by inhibiting the exchange of actin-bound nucleotide. Under low ionic strength conditions, the approximate dissociation constant (K_D) for the ADF–actin complex determined from exchange of nucleotide (1,N^6-etheno-ATP) is about 150 nM and is calcium-independent. Addition of ADF to monomeric actin inhibits actin assembly as well as the ATP hydrolysis that normally accompanies assembly. Complex formation is demonstrated between ADF and actin containing either ATP, ADP, or AMPPNP as the bound nucleotide. A K_D of 0.1–0.2 μM was calculated for both the ADF–ATP–actin and ADF–AMPPNP–actin complexes, whereas the K_D for the ADF–ADP–actin complex is about 1.3 μM. ADF can either depolymerize or cosediment with F-actin in a stoichiometric fashion, but these reciprocal activities are pH-dependent. At pHs between 6.5 and 7.1, ADF cosediments with F-actin and demonstrates only weak depolymerizing activity. ADF binding is cooperative and saturates at a 1:1 ADF:actin molar ratio. At pHs between 7.1 and 7.7, ADF shows increasing depolymerizing activity and less F-actin binding. At pH 8.0, ADF depolymerizes F-actin in a stoichiometric manner. Both the F-actin binding and the depolymerizing activities of ADF are inhibited by phalloidin. At pH 8.0, substoichiometric quantities of ADF, but not ADF–actin complex, transiently enhance the nucleating ability of F-actin solutions in a calcium-insensitive manner, suggesting that ADF has a weak severing activity, but does not cap the filament ends in a manner that inhibits the restoration of the original filament number. We conclude from these results that ADF is a noncapping, calcium-independent, pH sensitive F-actin binding/severing protein which is capable of forming moderate affinity complexes with actin monomers in which the nucleotide exchange is inhibited. The significance of these findings to a presumed cellular role for ADF is discussed.

Nonmuscle cells maintain a pool of unpolymerized actin which is available for assembly when needed (Bray & Thomas, 1976; Heacock et al., 1984; Cassimeris et al., 1992). This actin monomer pool is generated and maintained by proteins that regulate actin assembly. These proteins have been classified according to their actin binding properties into several groups [see review by Pollard and Cooper (1986)], one of which contains monomer-sequestering proteins with a Ca^{2+}-independent severing activity. The focus of this paper is on a member of this group.

Actin depolymerizing factor (ADF)[1] was identified and isolated from embryonic chick brain on the basis of its ability to rapidly depolymerize F-actin *in vitro* (Bamburg et al., 1980; Giuliano et al., 1988). Proteins with similar effects on actin have been identified in protists (Cooper et al., 1986), echinoderms (Mabuchi, 1983), and mammals (Berl et al., 1983; Maekawa et al., 1984; Nishida et al., 1984); recently, cDNAs made from plant pollen mRNA have been identified as encoding a family of ADF-related proteins (Kim et al., 1993). Sequence comparisons of these proteins show that chick ADF is a homolog (>95% homology) of porcine and human destrin (Abe et al., 1990; Adams et al., 1990; Moriyama et al., 1990). ADF also has substantial homology (70%) to porcine or chicken cofilin (Matsuzaki et al., 1988; Abe et al., 1990), and to yeast cofilin, an essential protein of the yeast cortical actin cytoskeleton (Moon et al., 1993). ADF, destrin, and cofilin are more closely related (especially in the presumptive actin binding domain) to the amoeba protein actophorin (Quirk et al., 1993) than they are to the echinoderm protein depactin (Takagi et al., 1988).

ADF is widely distributed among tissues of the chick (Bamburg & Bray, 1987). While in some tissues and cultured cell lines the levels of ADF alone may be sufficient to account for much of the unpolymerized actin (Bamburg & Bray, 1987; Koffer et al., 1988), in others ADF levels are far too low. The physical and chemical properties of chick brain ADF, as well as its ability to rapidly depolymerize F-actin and form a 1:1 complex with actin monomer, have been described (Bamburg et al., 1980; Giuliano et al., 1988; Harris et al., 1982). However, a more detailed quantitative characterization of its interactions with G- and F-actin is required to assess the role ADF plays in regulating actin assembly in cells. In this paper, we provide evidence that ADF binds cooperatively to F-actin

† Supported in part by NIH Grants GM35126, NS28338, NS28343, and TW01856 to J.R.B.

* Address correspondence to this author at the Department of Biochemistry, Colorado State University, Fort Collins, CO 80523. Phone: (303) 491–0425. FAX: (303) 491–0494.

‡ Present address: Department of Biochemistry, Biophysics and Genetics, University of Colorado Health Science Center, Denver, CO 80262.

• Abstract published in *Advance ACS Abstracts*, September 1, 1993.

[1] Abbreviations: ADF, actin depolymerizing factor; rADF, recombinant actin depolymerizing factor [contains three additional amino acids (Met-Gly-Ser-) N-terminal to the normally initiating Met]; SDS–PAGE, sodium dodecyl sulfate–polyacrylamide gel electrophoresis; ϵATP, 1,N^6-etheno-ATP; pyrenylactin, actin modified at Cys-374 with *N*-(1-pyrenyl)iodoacetamide; NBD–actin, actin modified at Cys-374 with *N*-ethylmaleimide and at Lys-373 with 7-chloro-4-nitro-2,1,3-benzoxadiazole; AMPPNP, 5′-adenylyl imidodiphosphate; DTT, dithiothreitol; EGTA, [ethylenebis(oxyethylenenitrilo)]tetraacetic acid; DNase I, bovine pancreatic deoxyribonuclease I; Pipes, piperazine-*N*-*N*′-bis(2-ethanesulfonic acid); Hepes, 4-(2-hydroxyethyl)-1-piperazine ethanesulfonic acid.

0006-2960/93/0432-9994$04.00/0

in a pH-dependent manner and that, at permissive pHs, ADF can sever F-actin and sequester actin monomers in a calcium-independent manner. In addition, we have determined that ADF protects monomeric actin from EDTA-induced denaturation by inhibiting nucleotide loss, and have quantified the interaction of ADF with actin containing different nucleotides. These results, some of which contradict findings reported for the mammalian ADF homolog destrin (Nishida et al., 1985; Moriyama et al., 1992), are useful in planning further studies on the behavior of ADF in cells.

MATERIALS AND METHODS

Materials. Red and Green A Dye-matrex resins were obtained from Amicon Corp. *N*-(1-Pyrenyl)iodoacetamide (pyrenyl) and 7-chloro-4-nitro-2,1,3-benzoxa-1,3-diazole (NBD) were obtained from Molecular Probes. [^{3}H]Cytochalasin B and [γ-^{32}P]ATP were obtained from New England Nuclear. 1,N^6-Ethenoadenosine 5′-triphosphate (ϵATP), *N*-ethylmaleimide (NEM), cytochalasin B, adenosine 5′-diphosphate (ADP), 5′-adenylyl imidodiphosphate (AMPPNP), phalloidin, and protein A–Sepharose were from Sigma Chemical Co. All other chemicals were analytical-grade reagents.

Purification of Proteins. Unless otherwise stated, all purified proteins were quick-frozen in liquid nitrogen in 100-μL aliquots and stored at −70 °C. Actin depolymerizing factor (ADF) was purified from frozen 18-day-old embryonic chick brains as previously described (Giuliano et al., 1988) and frozen in 10 mM Tris, pH 7.5, 0.5 mM DTT, and 1 mM NaN_3 (ADF buffer). Bacterially expressed recombinant ADF (rADF) was obtained as previously described (Adams et al., 1990). Skeletal muscle actin was purified from acetone powder of rabbit dorsal muscles (Pardee & Spudich, 1982) with further purification by gel filtration on Sephadex G-150. Aliquots were frozen in buffer G (2 mM Tris, pH 8.0, 0.2 mM $CaCl_2$, 0.5 mM DTT, 0.5 mM ATP, and 1 mM NaN_3). Profilin was isolated from 18-day-old embryonic chick brain by chromatography on poly(L-proline)–Sepharose (Tanaka & Shibata, 1985) and DEAE-cellulose in 2 M urea (Carlsson et al., 1977). Serum gelsolin was isolated from equine blood using a procedure (Harris & Gooch, 1981) modified to include Red Dye-matrex and protein A–Sepharose columns. It was kept on ice in the cold until used.

Modification of Proteins. Actin was labeled with *N*-(1-pyrenyl)iodoacetamide (Cooper et al., 1983). NBD–actin was prepared as described by Detmers et al. (1981). Both modified forms of monomeric actin were frozen in buffer G. The concentration of pyrenylactin and the degree of pyrene labeling were determined according to the method of Cooper et al. (1983). The degree of NBD labeling of NEM-treated actin was calculated using a molar extinction coefficient of 26 000 $M^{-1}cm^{-1}$ at 480 nm (Aboderin et al., 1973). ADP–actin was prepared according to the procedure of Lal et al. (1984). AMPPNP–actin was prepared by depleting ADP–actin of unbound nucleotide with two treatments of Dowex-1-Cl (20% v/v of a 50% suspension in buffer G without ATP) followed by addition of AMPPNP to 0.2 mM. Each treatment with Dowex-1-Cl involved a 5-min incubation followed by low-speed centrifugation for 2 min to remove the ion-exchange resin.

Protein Determination. Protein concentrations were determined spectrophotometrically using values of $E^{1\%} = 6.3$ at 290 nm for G-actin (Houk & Ue, 1974) and $E^{1\%} = 6.45$ at 280 nm for ADF (Giuliano et al., 1988). All other protein concentrations were determined using ovalbumin as a standard either in solution (Bradford, 1976) or after application to filter paper (Minamide & Bamburg, 1990).

Polyacrylamide Gel Electrophoresis. Sodium dodecyl sulfate–polyacrylamide gel electrophoresis (SDS–PAGE) on 12.5% or 15% gels was performed as decribed by Laemmli (1970) in mini-slab gels (Idea Scientific) (Matsudaira & Burgess, 1978). Samples for electrophoresis were prepared by boiling for 2 min after the addition (1:4) of 4× sample preparation buffer (0.25 M Tris, pH 6.8, 8% SDS, 40% glycerol, and 70 mM DTT). Proteins were stained with 0.5% Coomassie Blue R in 50% methanol/10% acetic acid and destained in the same solvent. For quantitative measurements of ADF and actin, gels were run with internal standards of ADF (0.2–1.6 μg) and actin (0.4–3.2 μg). Densitometry of bands was performed by computer integration of video images obtained with a cooled CCD camera interfaced to a TRI Microscan 2000 Image Analysis computer (Technology Resource Incorporated).

Fluorescence Measurements. Fluorescence measurements were made with an SLM 4800 spectrofluorometer. The bandpass for excitation was set at 0.5 nm and that for emission at 8 nm. The following settings were used for excitation and emission wavelengths, respectively: pyrenylactin, 366 and 388 nm; NBD–actin, 470 and 530 nm; 1,N^6-etheno-ATP, 350 and 410 nm.

Measurement of Monomeric Actin by DNase I Inhibition. This assay was performed according to the method of Blikstad et al. (1978) as modified by Heacock et al. (1982) on aliquots removed at various times from mixtures of G-actin in buffer G containing different molar ratios of ADF to actin. The denaturation of actin was initiated by the addition of EDTA to 2 mM. ADF treated independently with 2 mM EDTA retained its full ability to depolymerize F-actin at pH 8.0.

Nucleotide Exchange. A solution of G-actin (20 μM) in 2 mM Tris, pH 8.0, 0.05 mM $CaCl_2$, 0.125 mM ATP, 1 mM NaN_3, and 0.5 or 10 mM DTT was depleted of unbound nucleotide by treatment with Dowex-1-Cl as described for the preparation of AMPPNP–actin. After addition of ϵATP to 0.2 mM, the mixture was incubated for 1 h at 4 °C and again treated with Dowex-1-Cl as described. To prevent denaturation of the actin, ϵATP (18 μM) was added. For one set of experiments, the G-actin (5 μM) was mixed with different amounts of ADF (0–7 μM) in 2 mM Tris, pH 8.0, 0.05 mM $CaCl_2$ and 0.5 or 10 mM DTT. For a second set of experiments, ϵATP–G-actin (3 μM) was mixed with ADF (2 μM) in 2 mM Tris, pH 8.0, and 0.5 mM DTT containing different amounts of $CaCl_2$ (5.8, 50, 100, 150, 200, 250, and 500 μM). In all experiments, the exchange reaction was started by the addition of unlabeled ATP to 1 mM (at least 100-fold excess over ϵATP). Computer analyses of these and other data were performed on a MacIntosh IIsi with the KaleidaGraph software program (Abelbeck Software).

Determination of the Steady-State Actin Monomer Concentration. Changes in the fluorescence of pyrenylactin (Kouyama & Mihashi, 1981; Cooper et al., 1983) and NBD–actin (Detmers et al., 1981) were used to quantify actin assembly. Actin (NBD–ATP–actin, pyrenyl-ADP–actin, or pyrenyl-AMPPNP–actin) in buffer G was polymerized to steady state by the addition of KCl and $MgCl_2$ to 0.1 M and 2 mM, respectively. Different dilutions were made into buffer of identical composition, and the fluorescence intensities of the samples were measured after 4 h at 25 °C. The plots of fluorescence intensity vs concentration were extrapolated to a base-line curve (obtained from similar samples but in the absence of salts), and the concentration of actin at the intercept

was taken as the critical concentration. When performed in the presence of ADF, this assay measures the total amount of unpolymerized actin.

Measurement of ATP Hydrolysis. Unlabeled nucleotide on monomeric actin (63.4 μM) in buffer G (0.25 mM ATP) was exchanged for [γ-^{32}P]ATP (1.7 Ci/μmol; 1.8 μCi/mL) by overnight incubation. This labeled G-actin was incubated for 2 h with ADF or ADF buffer before the addition, at zero time, either of KCl of $MgCl_2$ to 0.1 M and 2 mM, respectively, or of an equal volume of water. The release of P_i was measured over time by the method of Martin and Doty (1949) as described by Pollard and Weeds (1984). Correction for free [^{32}P]P_i present in the [γ-^{32}P]ATP solutions was made by subtracting the amount of radioactivity extracted from samples in which G-actin was omitted.

Sedimentation Assay for ADF Binding and Depolymerization of F-Actin. G-Actin was dialyzed 4 h against 15 mM Pipes/15 mM Tris buffers ranging in pH from 6.5 to 8.0 and containing 0.2 mM ATP, and assembled for 30 min by the addition of $MgCl_2$ and KCl to 2 mM and 0.1 M, respectively (assembly buffers). In one set of experiments, actin in either 30 mM Pipes or 30 mM Hepes, both at pH 7.5, was used. Various amounts of ADF dialyzed against the same buffers were added to achieve the desired final molar ratios to actin, and after 30-min incubations at room temperature, an aliquot of each sample was removed for negative staining on electron microscope grids. The remainders of each sample (100 μL) were centrifuged for 30 min at 170000*g* in a Beckman airfuge in a 30° angle rotor. Temperature measurements of the samples before and after centrifugation showed fluctuations of less than ±3 °C, indicating that variations in pH due to the thermal effects on Tris (–0.03 pH unit/deg) will be less than 0.2 pH unit. Supernates were removed, and the pellets were washed once with assembly buffer. Both supernates and pellets were prepared for gel electrophoresis. ADF binding curves were corrected for the amounts of ADF which sedimented in the absence of actin (typically about 3% of the total ADF).

For quantitative studies on ADF depolymerization of F-actin, actin (10 μM final concentration) was assembled at room temperature for 30 min in 30 mM Tris, pH 8.0, containing 0.2 mM ATP, 0.5 mM DTT, 0.1 M KCl, and 2 mM $MgCl_2$ (final concentrations). Additions of ADF were made to achieve the desired final concentrations in a final volume of 50 μL. After 3-h incubation at room temperature, the samples were centrifuged at 170000*g* in a 10° angle rotor in the airfuge for 15 min. The supernate was mixed by gentle pipetting, and 40 μL was removed and prepared for SDS–PAGE by the addition of 10 μL of 5× sample preparation buffer. The remaining supernate was discarded; the pellet was rinsed with 50 μL of assembly buffer and then dissolved in 20 or 40 μL of 1× SDS–PAGE sample preparation buffer for analysis by SDS–PAGE. The amount of actin in the pellet was corrected for actin which sedimented from G-actin solutions incubated at room temperature for 3 h but without salt addition (about 10% of the total soluble actin pool).

The effects of phalloidin on both F-actin binding and F-actin depolymerizing activities of ADF were performed on actin assembled in either 30 mM Pipes, pH 6.8, or 30 mM Tris, pH 8.0, as described above, with 20 μM phalloidin added to the 10 μM actin either 10 min before or 10 min after the addition of ADF.

Electron Microscopy. Aliquots (5 μL) of ADF/actin mixtures were placed on glow-discharged 400-mesh, carbon-coated, formvar grids for 10 s. The sample was removed by diluting with drops of 1% uranyl acetate. After a few seconds, the uranyl acetate was removed by blotting with the torn edge of filter paper. Transmission electron microscopy was performed on a Philips 400 electron microscope with photographs taken at 5K and 15K magnifications.

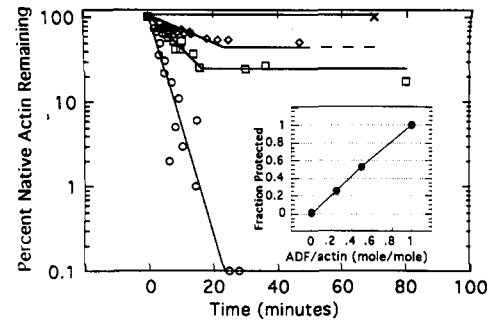

FIGURE 1: ADF protects actin from denaturation by EDTA. Prior to the addition of 2 mM EDTA, G-actin (5 μM final concentration) in G-actin buffer was incubated with different molar ratios of ADF to actin: (○) no ADF; (□) 0.25; (◇) 0.5; (×) 1.0. Starting at the time of EDTA addition, and at the time intervals shown thereafter, 10-μL aliquots of the mixture were assayed for inhibition of 2 μg of DNase I. The starting concentration of actin gave about 80% inhibition of the DNase activity and was taken as 100% of native actin remaining. INSET: Plot of the fraction of actin protected after 1 h in EDTA versus the molar ratio of ADF to actin.

Nucleating Ability of F-Actin Solutions. Pyrenyl-G-actin at pH 8.0 was polymerized to steady state at 25 °C by the addition of $MgCl_2$ to 1 mM. Aliquots of the resulting pyrenyl-F-actin solution were incubated for 2 min with ADF or ADF buffer and then added to a solution of pyrenyl-G-actin (3 μM, same extent of pyrene label) that had been preincubated for 1 min in buffer G plus 1 mM $MgCl_2$ (Wagner & Wegner, 1985). The assembly of 3 μM G-actin during the preincubation period was negligible. Addition of EGTA (pH 7.5) to all buffers was used to lower the Ca^{2+} concentration to 1.0×10^{-9} M, calculated using the apparent binding constant with adjustments made for pH (Harafuji & Ogawa, 1980; Harris & Weeds, 1983). In the absence of added EGTA, the Ca^{2+} concentration was 0.2 mM. All transfers involving F-actin solutions were made with large-bore (truncated) pipe tips to minimize mechanical shearing. The initial rates of assembly of G-actin samples mixed with F-actin in the absence of ADF was taken as 100%.

Cytochalasin B Binding to ADF-Treated and Gelsolin-Treated F-Actin. Actin, polymerized to steady state in 0.1 M KCl and 2 mM $MgCl_2$, was incubated with varying amounts of ADF or equine serum gelsolin in the presence of 1.0 mM $CaCl_2$. Samples were dialyzed for 30 h to equilibrium against 5 mM Tris, pH 8.0, 50 mM KCl, 1 mM $MgCl_2$, 1 mM $CaCl_2$, 0.2 mM ATP, 0.5 mM DTT, and 1.5 mM NaN_3 containing 40 nM [^{3}H]cytochalasin B (1.0 Ci/mmol) (Lees et al., 1984). Dialysis was performed in a multiwell microdialysis chamber (MRA Corp.). Aliquots from duplicate samples were removed, and the level of [^{3}H]cytochalasin B was quantified in a Beckman LS 7800 liquid scintillation counter. The amount of [^{3}H]cytochalasin B that was not displaced by a 1000-fold excess of unlabeled cytochalasin B was taken as a measure of nonspecific binding.

RESULTS

Protection of Actin from Denaturation by EDTA. The protective effect of ADF on actin denaturation induced by 2 mM EDTA is shown in Figure 1. Complete protection of the fraction of actin associated with ADF is achieved for at least 1 h (Figure 1, inset), and this stoichiometry, coupled with previous studies showing an ADF–actin complex of 60 kDa

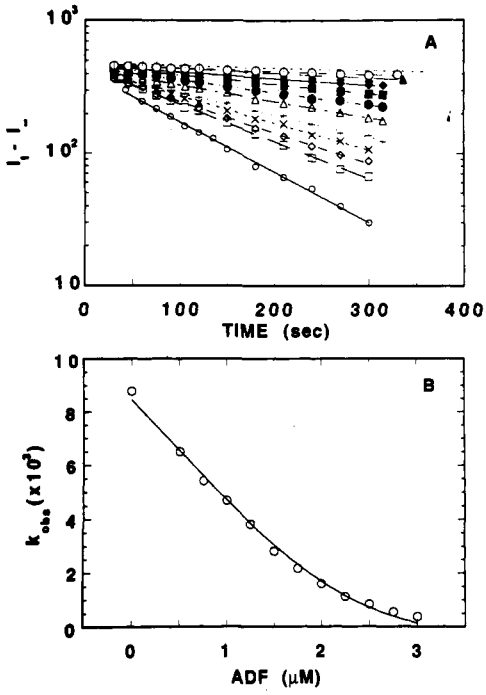

FIGURE 2: Effect of ADF on the exchange rate of actin-bound nucleotide. (A) The exchange of ϵATP bound to G-actin (5 μM) with unlabeled ATP (1 mM) was followed over time in the presence of ADF buffer (lower curve) or ADF (increasing concentrations of 1.0, 1.5, 2.0, 2.5, 3.0, 3.5, 4.0, 4.5, 5.0, 5.5, 6.0, 6.5, and 7.0 μM). The DTT concentration in all buffers was 0.5 mM. The fluorescence intensity for each time point was corrected by subtraction of the fluorescence intensity at steady state (3 h) and the logarithm of the difference plotted against time. The slopes of these lines are the exchange rate constants (k_{obs}). (B) Plot of the k_{obs} values from (A) versus the ADF concentration. The line represents the best computer fit of these data to the nucleotide exchange equation (Bryan, 1988) which gave a value for the K_D of the ADF–actin complex of 0.15 μM.

on gel filtration (Giuliano et al., 1988), confirms a 1:1 interaction. The rate constant for the pool of actin that denatures is 0.001 ± 0.0006 s^{-1} in the presence or absence of ADF. Since recent studies have shown that EDTA-induced denturation of actin results from nucleotide loss that follows metal ion depletion (Miki, 1991), our results imply that the the dissociation rate of nucleotide is slow compared to the time ADF occupies its binding site and that each ADF cannot protect more than a single actin.

Effects of ADF on Actin Nucleotide Exchange. The interaction of binding proteins with actin monomer can alter the rate of nucleotide exchange from the actin and can provide a convenient method for measuring the amount of complex under equilibrium binding conditions (Mockrin & Korn, 1980; Nishida, 1985). Nucleotide exchange is most readily measured by using 1,N^6-etheno-ATP (ϵATP), an ATP analog which is fluorescent when bound to actin (Miki et al., 1974). Dilution of G-actin containing bound ϵATP into buffer containing a 100-fold excess of ATP resulted in a first-order decline in fluorescence, the rate of which was inhibited by incubation of the actin with ADF prior to dilution (Figure 2A). The rate constants for the exchange of nucleotide in the presence of ADF (k_{obs}) were plotted against the ADF concentration (Figure 2B). This plot was fitted to the rate equation for actin nucleotide exchange in the presence of actin binding proteins (Bryan, 1988). A best fit for these data is obtained with a dissociation constant (K_D) of 0.15 μM. This experiment has been repeated several times using different concentrations of reducing agents (0.5 or 10 mM DTT) and different preparations of actin and ADF. The K_Ds calculated from

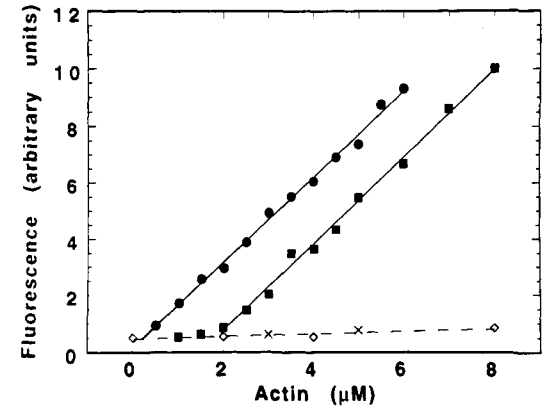

FIGURE 3: ADF shifts the critical concentration of actin by sequestering actin. NBD–actin (78% NBD) was polymerized to steady state by the addition of KCl and $MgCl_2$ to 0.1 M and 2 mM, respectively. Different dilutions of NBD–F-actin were made in the presence of ADF buffer (●) or 2.5 μM ADF (■). The fluorescence intensity was measured at 25 °C after 4 h. Base-line values were obtained from similar samples but without the addition of salts in the absence (◊) or presence (×) of 2.5 μM ADF.

these experiments fell between 0.1 and 0.45 μM, with an average of 0.2 μM. Since nucleotide exchange on G-actin is highly dependent on calcium ion concentration (Frieden & Patane, 1988; Nowak et al., 1988), we evaluated the effects of ADF on the nucleotide exchange process at seven different calcium concentrations from 5.8 to 500 μM. A single concentration of ADF (2 μM) was used which reduced the exchange rate on 5 μM G-actin by 50% at 50 μM calcium. Although the exchange rate for the actin-bound nucleotide varied significantly over the range of calcium concentrations used [data not shown; see Frieden and Patane (1988) and Nowak et al. (1988)], the extent of inhibition by ADF was identical (50% reduction in exchange rate) under all conditions. Thus, the interaction of ADF with G-actin is independent of calcium concentration, and the degree of inhibition of actin nucleotide exchange by ADF is independent of the rate of exchange.

Dissociation Constant for the Actin–ADF Complex Formed under Actin Assembly Conditions. Different dilutions of pyrenylactin or NBD–actin were made into buffer without salts, or into assembly buffers in the presence and absence of 2.5 μM ADF and polymerized to steady state at pH 8.0. Figure 3 shows typical results from which the concentration of unassembled actin in the presence and absence of ADF was calculated by extrapolation of the curves to the base line (absence of added salts). The K_D for the actin–ADF complex is calculated from the data in Figure 3 using eq 1 where $[A_f]$is

$$K_D = [A_f][D_f]/[DA] \approx [G_0][DT-DA]/[DA] \quad (1)$$

the free actin concentration, $[D_f]$ is the free ADF concentration, [DA] is the concentration of actin–ADF complex, $[G_0]$ is the actin critical concentration, and [DT] is the total ADF concentration. The concentration of complex (DA) is taken as the shift between the two curves in Figure 3. In separate experiments using either NBD–actin or pyrenylactin, K_Ds between 0.09 and 0.16 μM were obtained, even when assembly conditions were varied to give over a 9-fold difference in critical concentration (Table I). The apparent K_D is unaffected by altering the salt conditions from buffer G containing 0.1 M KCl and 2 mM $MgCl_2$ to buffer G containing only 0.6 mM $MgCl_2$ and is also independent of the degree of fluorochrome label on the actin. Thus, the affinity of ADF for actin is not affected significantly either by fluorochrome

Table I: Dissociation Constants for the Actin–ADF Complex Determined under Different Conditions

actin fluorescence label	actin-bound nucleotide	ionic conditions	actin critical concn (μM)	dissociation constant (μM)
78% NBD	ATP	0.1 M KCl, 2 mM $MgCl_2$	0.12	0.16
78% NBD	ATP	0.1 M KCl, 2 mM $MgCl_2$	0.15	0.14
49% pyrene	ATP	0.1 M KCl, 2 mM $MgCl_2$	0.18	0.09
34% pyrene	ATP	0.6 mM $MgCl_2$	1.13	0.11
25% pyrene	ADP	0.1 M KCl, 2 mM $MgCl_2$	2.25	1.26
25% pyrene	AMPPNP	0.1 M KCl, 2 mM $MgCl_2$	0.30	0.11

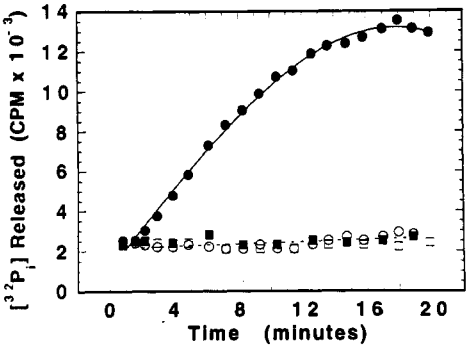

FIGURE 4: ADF inhibits ATP hydrolysis by actin. [γ-^{32}P]ATP–G-actin (4.8 μM) was polymerized by the addition of KCl and $MgCl_2$ to 0.1 M and 2 mM, respectively, in the absence (●) or presence of 8.7 μM ADF (□). The release of radioactive phosphate was measured. Control samples contained G-actin in the absence of added salts and in the presence (■) or absence (○) of ADF.

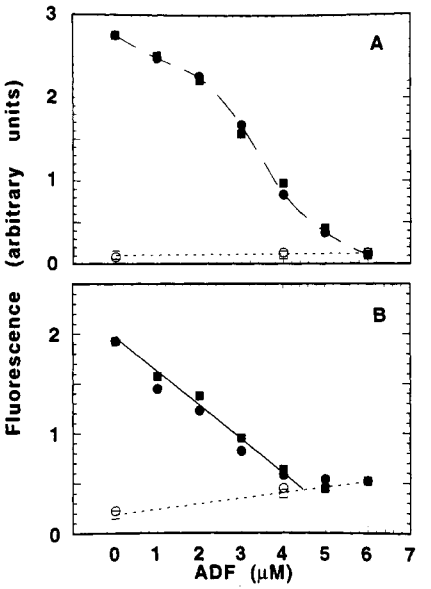

FIGURE 5: Depolymerization of F-actin by titration with ADF. (A) Pyrene–G-actin [6.3% pyrene (●) or 67% pyrene (■)] was polymerized by the addition of KCl and $MgCl_2$ to 0.1 M and 2 mM, respectively. ADF or ADF buffer was then added. The final concentration of actin in both experiments was 4 μM. After 4 h, the fluorescence of the samples was determined. Base-line values were obtained from identical samples but without added salts. (B) Conditions were identical to those described in (A). F-Actin (4 μM) was labeled with 7.6% NBD (●) or 77% NBD (■). Base-line values were obtained from identical samples but without added salts.

modification of actin or by changes in ionic strength between about 10 and 220 mOsm.

Interaction of ADF with Actin Containing Different Bound Nucleotides. The effect of ADF on the hydrolysis of ATP by actin under different ionic conditions is shown in Figure 4. ADF does not stimulate the negligible rate of ATP hydrolysis which occurs with G-actin alone. A molar excess of ADF completely inhibits the rate increase observed upon addition of salts (0.1 M KCl and 2 mM $MgCl_2$, final concentration) to the G-actin. Thus, the inhibition of actin assembly by ADF also inhibits the ATP hydrolysis which normally accompanies actin assembly. At pH 8.0, ADF depolymerizes pyrenylactin filaments containing either ADP or AMPPNP as the only nucleotide, yielding K_Ds of 1.26 and 0.11 μM, respectively (Table I). Thus, nucleotide hydrolysis is not necessary for ADF activity.

Depolymerization of F-Actin by Titration with ADF. The fluorescence of pyrenyl-F-actin is decreased by addition of ADF. The drop in fluorescence is rapid, a new steady-state level being reached in about the time it takes to mix the ADF and actin. However, the ADF titration curve for pyrenylactin depolymerization is sigmoidal in shape (Figure 5A). This sigmoidicity is not due to ADF preferentially binding to the unlabeled form of actin since identical curves were obtained using actin modified to 6.3% or 67% with pyrene. However, depolymerization of NBD–F-actin is linear and directly proportional to ADF concentration (Figure 5B), regardless of the extent of modification with NBD. The reason for the different results for actin modified with the two fluorochromes is unclear, but the results may indicate that ADF has a more complex interaction with pyrenylactin (either monomer or polymer) which impacts the final fluorescence.

pH Dependence of ADF Binding and Depolymerizing F-Actin. The pH dependence of the cosedimentation of ADF with F-actin is apparent from the results of SDS–PAGE shown in Figure 6A. To quantify ADF binding to F-actin at different pHs while keeping the major components of the solution constant, we repeated this experiment with varying concentrations of recombinant ADF (rADF) and 5 μM actin in a series of buffers containing both 15 mM Tris and 15 mM Pipes at 0.3 pH unit intervals between 6.5 and 8.0. Standard curves run internally on each gel ensured that quantitative measurements of both rADF and actin were obtained within the linear range. At pHs below 7.1, rADF binds to F-actin (Figure 6B), and has low (but measurable) depolymerizing activity (Figure 6C). At pH 8, rADF no longer sediments with F-actin and has maximal depolymerizing activity (Figure 6B, C). Both activities were evident throughout the intervening pH range and electron microscopy (not shown) gave qualitative confirmation of these results. Identical binding curves were obtained at pH 7.5 in either Pipes buffer or Hepes buffer (data not shown). Replotting the binding results obtained using a 2.5 molar excess of rADF along with the percent of actin depolymerized at each pH shows the reciprocal relationship between F-actin binding and depolymerization (Figure 7). The largest increase in depolymerizing activity and the largest decrease in rADF binding to F-actin occur between pH 7.1 and 7.4.

The binding of rADF to F-actin at pH 6.8 was studied in more detail using 10 μM F-actin. The cooperative nature of the rADF binding is evident in Figure 8A. Pellets were

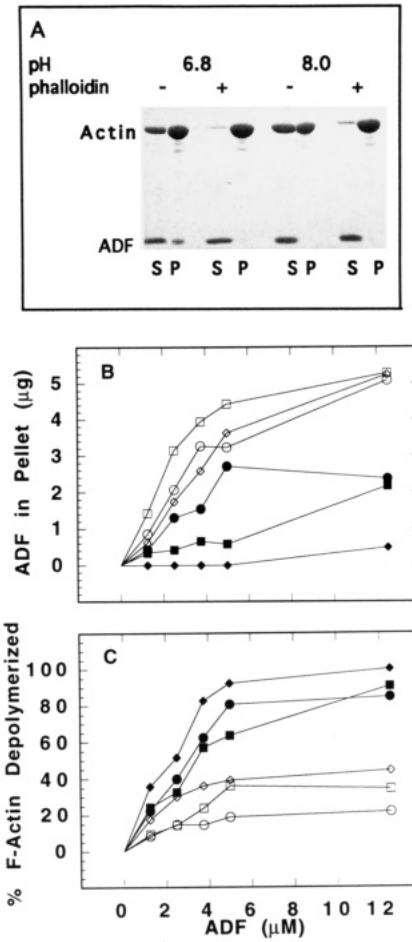

FIGURE 6: Effect of pH on the cosedimentation of ADF and F-Actin. F-Actin (5 μM final concentration) in 15 mM Pipes/15 mM Tris buffers containing 2 mM $MgCl_2$ and 0.1 M KCl at the pHs shown was incubated with different amounts of ADF, and after 30 min, the samples were centrifuged at 170000g for 30 min. The supernate was removed, and the pellets were rinsed with the buffer and then resuspended in 40 μL of sample preparation buffer for SDS–PAGE. The ADF and actin in each sample were quantified by densitometric analysis of Coomassie Blue-stained gels containing ADF and actin standards. (A) Representative gel showing supernate (S) and pellet (P) fractions of the actin sample incubated with 0.5 mol of ADF/mol of actin at pH 6.8 and 8.0 in the presence (+) or absence (–) of 20 μM phalloidin. (B) ADF in the pellet fraction of actin assembled at different pHs in the presence of differing ADF concentrations. Values are corrected for the amount of ADF sedimenting in the absence of F-actin (less than 3% of total ADF in pellet). pH 8.0 (♦); pH 7.7 (■); pH 7.4 (●); pH 7.1 (◊); pH 6.8 (□); pH 6.5 (○). (C) Percent of F-actin depolymerized by ADF at the different pHs. Symbols identical to those in (B).

resuspended in small volumes of buffer for gel analysis so that a level of rADF equal to 1% or more of the actin could have been detected and quantified if present. This binding study was repeated using brain ADF and 5 μM actin, and the molar ratio of ADF to actin in the pellet fractions was calculated by quantifying both ADF and actin in the same samples (Figure 8B). This ratio reaches a maximum of 1:1 even at a 2.5 molar excess of ADF. A Hill plot of these binding data (Figure 8B, inset) is linear with a Hill coefficient of 2.5 determined by computer fit of the data to the Hill equation. Addition of profilin (2–10 μM) had no effect on ADF binding and cosedimenting with F-actin; however, 20 μM phalloidin added prior to the ADF completely inhibited ADF binding (Figures 6A and 8B).

The depolymerizing activity of ADF was studied in more detail using the sedimentation assay. Incubation of 10 μM F-actin with increasing concentrations of ADF at pH 8.0 results

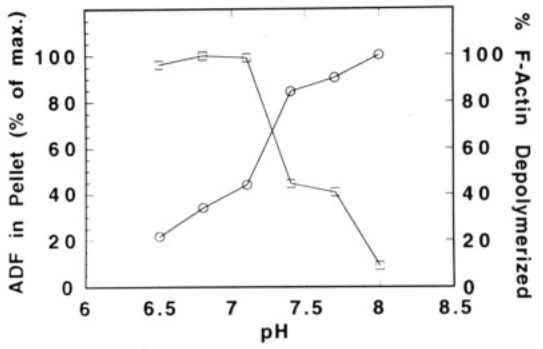

FIGURE 7: Effects of pH on the actin depolymerizing activity of ADF and the binding of ADF to F-actin. Amounts of ADF and actin in pellet and supernate fractions were obtained from the SDS–PAGE analysis of experiments shown in Figure 6B,C in which 5 μM F-actin was incubated with a 2.5 molar excess of ADF. ADF in the pellet (□) is expressed as the percent of the maximum (occurring at pH 6.8 or 7.1) and is corrected for ADF sedimenting in the absence of actin. The fraction of actin depolymerized (○) is corrected for G-actin which pellets in the absence of salts.

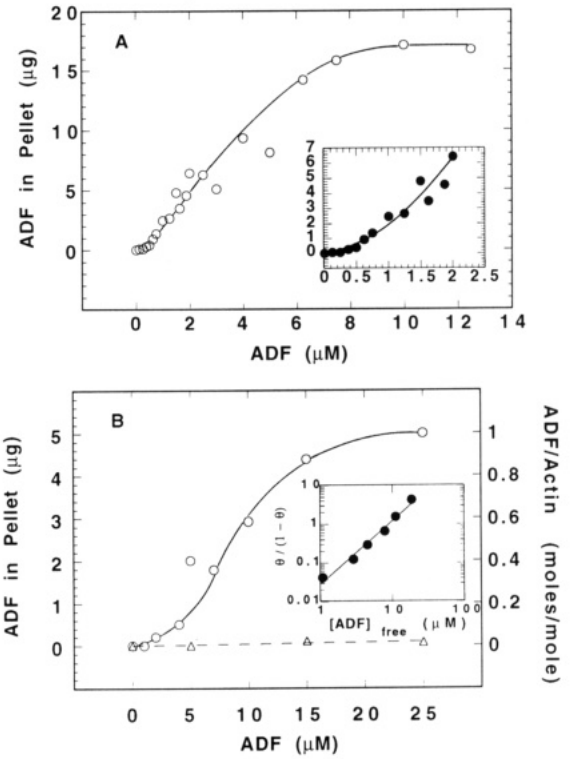

FIGURE 8: Binding of ADF to F-actin at pH 6.8. (A) F-Actin (10 μM final concentration) was incubated at pH 6.8 in 15 mM Pipes/15 mM Tris containing 0.1 M KCl and 2 mM $MgCl_2$ with various concentrations of rADF (100-μL final volume), and the samples were centrifuged. The protein pellets were washed once with assembly buffer and solubilized in SDS–PAGE sample preparation buffer. ADF and actin were quantified as described under Materials and Methods. Data are from four separate experiments. INSET: Expanded plot of the data at lower rADF concentrations. (B) Similar experiment to that described above but done with 5 μM F-actin and brain ADF in a 50-μL final volume. The molar ratio of ADF to actin in the pellet fraction is also plotted. (△) Binding experiment in which the F-actin was incubated with 20 μM phalloidin prior to the addition of the ADF. INSET: Hill plot of these binding data. The occupied sites (θ) were taken as the moles of ADF per mole of actin in the pellet. The free ADF concentration was taken as that remaining in the supernate fraction. The slope of this plot is the Hill coefficient, the best fit being 2.5.

in complete depolymerization of the actin (Figure 9). Electron microscopic observations of these samples confirmed the absence of actin filaments at ADF concentrations above 10 μM. This depolymerization curve could be fit to the transform

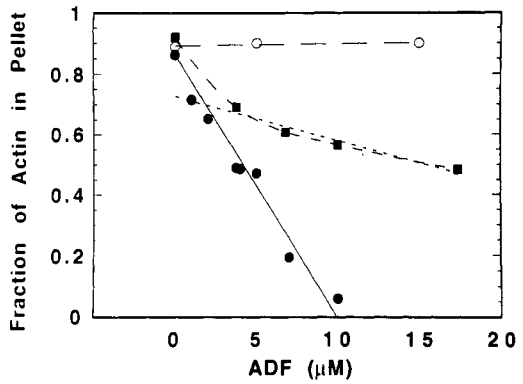

FIGURE 9: Depolymerization of F-actin by ADF as measured by sedimentation. (●) Actin (10 μM) was assembled with salts at pH 8.0 as described under Materials and Methods. After 30 min, ADF was added to give the concentrations shown. After 3 h, the samples were centrifuged, and the actin in the supernate and pellets was quantified. The solid line is a computer fit to eq 2 and gives a K_D = 0.17 μM. (○) Data for experiments in which 20 μM phalloidin was added either 10 min prior to or 10 min after addition of ADF at pH 8.0. (■) Actin (13.6 μM) was assembled with salts at pH 6.8. ADF was added after 30 min and after 3 h, the samples were centrifuged, and the actin in the supernate and pellets was quantified. The ADF concentration shown is that calculated for the supernate (total ADF minus that pelleted with F-actin). The dashed straight line is the best computer fit of the data to eq 2, giving a new critical concentration of actin (3.76 μM) and a K_D for the ADF–actin complex of 16.1 μM.

of the expression for K_D (eq 1):

$$A_f = \{A_t - G_0 - [P_t/(1 + K_D/G_0)]\}/A_t \qquad (2)$$

which states that the fraction of assembled actin (A_f) is dependent on the critical actin concentration (G_0), the total actin concentration (A_t), the total monomer binding protein concentration (P_t), and the K_D of the complex (Tobacman & Korn, 1982). The dissociation constant which best fits these data is 0.171 μM, a value consistant with those derived from other methods reported above. Addition of 20 μM phalloidin to the actin, either before or after the ADF, completely inhibits the increase in the actin monomer pool, demonstrating that phalloidin both can protect the actin from ADF-induced depolymerization and can drive the assembly of F-actin from the ADF–actin complex (Figure 9). No ADF appeared in the F-actin pellets obtained at pH 8.0 in the presence of phalloidin (Figure 6A).

At pH 6.8, ADF cosediments with actin filaments and demonstrates only weak depolymerizing activity. In Figure 9, the fraction of actin in the pellet is plotted against the ADF concentration remaining in the supernate. The resulting curve best fits a model in which (1) ADF binding to F-actin increases the critical concentration (presumably by altering the off- or on-rates at the filament ends) and (2) the ADF demonstrates a much reduced affinity for the actin monomer in solution. The best fit of these data to eq 2 gives a K_D of 16.1 μM, 2 orders of magnitude weaker binding to actin monomer than is observed at pH 8.0. Alternatively, actin may be severed by ADF at pH 6.8, and the smaller actin fragments and associated ADF may not sediment completely under our conditions. Other assays to evaluate these alternatives need to be done.

ADF Has a Weak F-Actin Severing Activity. The elongation rate of pyrenylactin assembly induced by 1 mM $MgCl_2$ is slightly faster in the presence of substoichiometric amounts of ADF (0.23 mol/mol of actin) than in its absence (Koffer et al., 1988). However, the presence of ADF also produces a slightly longer lag period and the expected inhibition in the final extent of actin assembly. These assembly kinetics suggest that ADF is capable of severing newly formed pieces of F-actin,

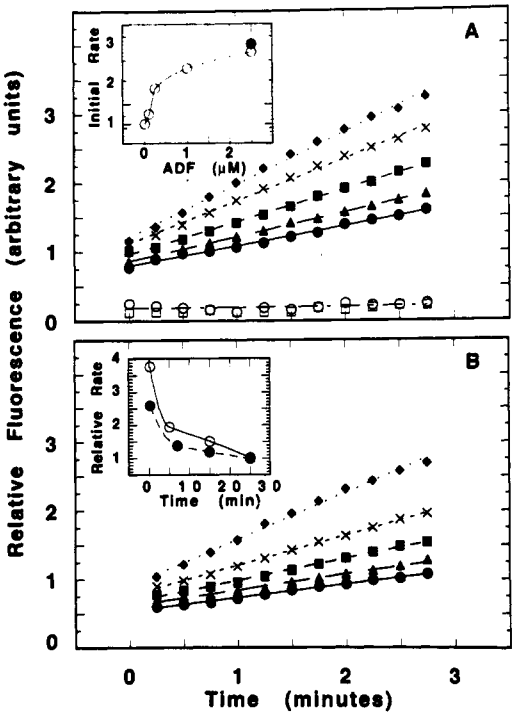

FIGURE 10: ADF severs actin filaments but does not prevent filament number redistribution after severing. (A) Pyrene–G-actin (14.4 μM; 30% pyrene) was polymerized at 25 °C for 2 h in buffer G plus 1 mM $MgCl_2$. Samples of the F-actin were incubated with varying amounts of ADF or ADF buffer for 2 min such that the final concentration of F-actin was 10.7 μM and that of ADF was 0 (●), 0.12 (▲), 0.24 (■), 0.96 (×), or 2.4 μM (♦). At zero time, pyrenylactin monomers (30% pyrene; 3.0 μM), preequilibrated for 1 min with buffer G plus 1 mM $MgCl_2$, were added, and the fluorescence was followed over time. At zero time, [pyrene–G-actin] = 2.62 μM and [pyrene–F-actin] = 1.40 μM. Assembly of pyrene–G-actin in the absence of both pyrene–F-actin and ADF (○), and in the absence of pyrene–F-actin but with the addition of 1.2 μM ADF (□). INSET: relative initial rate of assembly versus the ADF concentration under conditions that included 2.0×10^{-4} M Ca^{2+} (○) or 2.0×10^{-4} M Ca^{2+} plus 1 mM EGTA (●). Values obtained in the absence of ADF were taken as 1.0. (B) Pyrene–F-actin (12.5 μM; 40% pyrene) was incubated with ADF buffer (●) or with 3.1 μM ADF for 0.5 (♦), 5 (×), 15 (■); and 25 min (▲) at which times aliquots were removed and assayed for their ability to nucleate assembly of pyrene–G-actin (3 μM; 40% pyrene). At zero time, [pyrene–G-actin] = 2.60 μM and [pyrene–F-actin] = 1.62 μM. Results shown were obtained in the presence of 0.2 mM Ca^{2+}. INSET: relative initial rate of assembly versus the time of incubation for the pyrene–F-actin/ADF solution under conditions of 2.0×10^{-4} M Ca^{2+} (○) or 2.0×10^{-4} M Ca^{2+} plus 1 mM EGTA (●).

creating additional sites of nucleation that enhance the rate of polymerization, but that ADF also removes some G-actin from the assembly-competent pool, thus taking longer to achieve the initial nucleation steps, i.e., a longer lag phase. Additional evidence for F-actin severing at pH 8.0 by ADF was obtained by measuring the ability of an F-actin solution to nucleate assembly of G-actin (Nishida et al., 1984) before and after treatment with different concentrations of ADF (Figure 10A). When measured soon after treatment with ADF, the nucleating capacity of the F-actin is enhanced in a manner dependent upon ADF concentration (Figure 10A, inset). However, the nucleating ability of the ADF-treated F-actin solution declined over time, approaching that of the untreated F-actin within 25 min after ADF addition in either the presence or the absence of calcium (Figure 10B). Previous studies with the porcine analog of ADF (destrin) reported that the enhanced nucleating ability of the severed filaments was long-lived (Nishida et al., 1984). If this were the case for ADF, one might be able to demonstrate enhanced

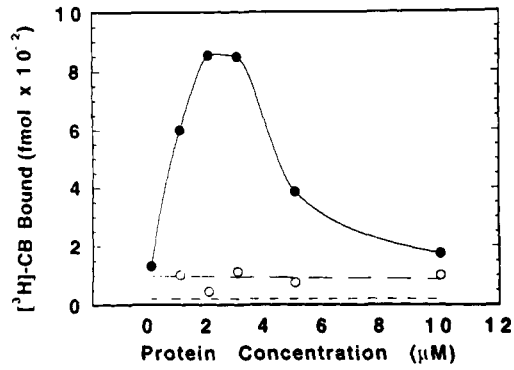

FIGURE 11: Binding of cytochalasin B to F-actin in the presence of serum gelsolin or brain ADF. F-Actin (11.6 μM) was mixed with the indicated amounts of serum gelsolin (●) or ADF (○) in the presence of 0.5 mM $CaCl_2$ followed by equilibrium dialysis against polymerization buffer containing 40 nM [^{3}H]cytochalasin B (1.0 Ci/mmol). Values plotted are the averages of duplicate samples minus the amount of [^{3}H]cytochalasin B in the dialysis buffer at equilibrium. The dashed line at the bottom of the graph represents nonspecific binding of [^{3}H]cytochalasin B.

cytochalasin B binding to filament ends as shown previously for other actin severing and capping proteins (Lees et al., 1984). As an internal control for these experiments, we used the known severing and capping protein serum gelsolin (brevin) (Harris & Schwartz, 1981). Enhanced cytochalasin B binding was observed for F-actin treated with serum gelsolin but not for F-actin treated with ADF (Figure 11). Thus, ADF does not prevent restoration of the original filament number distribution after severing.

DISCUSSION

Interactions of ADF with Monomeric Actin. Previous studies have shown that actin denatured by heating loses with identical kinetics its ability both to assemble into filaments and to inhibit DNase I (Heacock et al., 1982). Thus, the DNase I inhibition assay is a sensitive method for quantifying actin denaturation. In addition, the binding of actin to DNase I inhibits further actin denaturation induced by EDTA (Miki, 1991). The similar rate constants obtained here for actin denaturation in the absence of ADF and in the presence of substoichiometric amounts of ADF suggest that only the actin within the complex is protected from denaturation. Since the denaturation of actin induced by EDTA has been shown to result from the loss of nucleotide which follows metal ion depletion (Miki, 1991), it seemed logical to assume that ADF would inhibit nucleotide exchange. Such inhibition has previously been demonstrated for the actin binding proteins cofilin (Nishida, 1985), DNase I (Mannherz et al., 1980; Hitchcock, 1980), and thymosin β_4 (Goldschmidt-Clermont et al., 1992). The results reported here show ADF also inhibits this exchange. The K_D, calculated from analyses of the kinetics of nucleotide loss, varied from 0.10 to 0.45 μM under these low ionic strength conditions. Values at the lower end of this range are in good agreement with dissociation constants obtained here under more physiological conditions of ionic strength by a variety of other methods.

The weak dissociation constant for ADF and ADP–actin (K_D = 1.3 μM; Table I) is the one exception to the moderate affinities ($K_D \approx$ 0.1–0.2 μM) measured for all other ADF–actin complexes at either low or physiological ionic strengths. ADP–actin is the only form studied here that is unable to undergo the magnesium-induced conformational shift postulated to be required in monomer activation (Frieden & Patane, 1985; Barden & dos Remedios, 1985). Actin containing either ATP or AMPPNP, a nonhydrolyzable analog (Cooke & Murdoch, 1973), assembles identically (Cooke, 1975), demonstrating that nucleotide hydrolysis is not necessary for monomer activation. These findings suggest a model in which ADF binds preferentially to actin which is in the "activated monomer" conformation, the major form of both assembled and unassembled actin that should exist under intracellular conditions. If this is the case, then ADF may be able to induce this conformation upon binding *in vitro* to forms of G-actin that are capable of undergoing this conformational change. Further studies to evaluate this possibility need to be done.

Interactions of ADF with F-Actin. Although we previously showed that some ADF, when it was present at high concentrations in cell fractions, could cosediment with F-actin (Koffer et al., 1988), the significance of this finding was unclear. Since the isoelectric point for ADF is about 7.9 (Giuliano et al., 1988), it was considered likely that small amounts of this basic protein could bind and cosediment with an acidic polymer like actin. Other studies that failed to detect the pH dependence of ADF in depolymerizing F-actin either used lower concentrations of ADF and actin than were used here or only looked at the increase in actin released into the supernate which occurs to some degree even under conditions where much of the ADF cosediments with actin (Abe & Obinata, 1989; Bamburg et al., 1991). However, the cooperativity of the binding, its saturability at a 1:1 stoichiometry, and its relatively sharp pH dependence all suggest that this binding is specific. The reciprocal relationship observed between the F-actin binding and depolymerizing activities of ADF over the pH range of 6.5–8.0 is very similar to the activities previously reported for cofilin (Yonezawa et al., 1985). Given the high sequence similarity (about 70% homology) between ADF and cofilin, it is not unexpected that these similarities in activity exist, and indeed suggest that these two proteins may be considered isoforms generated by related genes.

It has been reported that the mammalian homolog of ADF (destrin) is insensitive to pH in its depolymerization of F-actin (Nishida et al., 1984; Moriyama et al., 1992). Using a sedimentation assay similar to that used here, Moriyama et al. (1992) could not detect sigificant binding of recombinant destrin to F-actin at pH 7.0. However, many different chimeric constructs between destrin and cofilin all showed F-actin binding at pH 7.0 with reduced binding or no binding at pH 8.3, similar to what we observed here for ADF. The only difference in the procedure between these studies is that Hepes was a component of the binding buffer used by Moriyama et al. (1992) and the samples were centrifuged at higher speeds, which should increase and not decrease the sedimentation of ADF–F-actin complexes. We show here that ADF binds identically to F-actin in either Hepes or Pipes. Hawkins et al. (1993) demonstrated that human ADF (identical in sequence with porcine destrin) shows cooperative pH-sensitive F-actin binding similar to what we observe with chick ADF. Thus, it is difficult to reconcile the differences reported between the pH-sensitive F-actin binding of ADF and destrin, other than to suggest that the additional nine amino acids on the N-terminus of the bacterial expressed destrin used in the studies of Moriyama et al. (1992) affected its pH-dependent F-actin binding, but not that of the chimeric proteins. Our recombinant ADF, which is expressed with three additional N-terminal amino acids, behaved identically to ADF isolated from brain in its pH-dependent F-actin binding (see Figure 8).

The ability of ADF to sever actin filaments is demonstrated by the enhanced ability of F-actin treated with ADF to nucleate assembly of G-actin. Similar studies done with the ADF analogs porcine destrin and starfish oocyte depactin (Nishida et al., 1984) demonstrated enhanced nucleation, but this effect persisted for many hours after the F-actin was treated with these proteins. In our hands, actin severed by ADF either reanneals (Murphy et al., 1988) or redistributes to approach the original filament number concentration within a short time. The ADF–actin complex neither severs F-actin nor hydrolyzes ATP, an activity which presumably would be required to serve as an energy source for continuous severing. Three ways in which these differences between ADF and the porcine destrin might be explained come to mind: (1) the porcine brain destrin differs in its activity from chick brain ADF; (2) the pH at which the severing assay was performed by Nishida et al. (1984) also allowed filament binding of ADF, and this binding serves to restrict reannealing or redistribution; or (3) actin capping proteins might have been present to prevent redistribution. Explanation 1 seems unlikely in view of recent studies with bacterially expressed human ADF (destrin) that show filament number redistribution occurs with kinetics similar to those observed here for chicken ADF (Hawkins et al., 1993). Explanation 2 is more difficult to assess. Our studies were done at pH 8.0 where ADF does not cosediment with F-actin while those of Nishida et al. (1984) were done at pH 7.5 where ADF can both depolymerize and cosediment with F-actin. No systematic study has been done to determine if ADF bound to F-actin affects filament reannealing or redistribution, although the increased critical actin concentration induced by ADF bound to F-actin at pH 6.8 (see Figure 9) suggests that the bound ADF may have such an effect. Explanation 3 is also possible since F-actin capping proteins are plentiful in brain [see review by Bamburg and Bernstein (1991)] and only small amounts of such a protein would be required to prevent filament redistribution following severing.

Role of ADF in Modulation of Actin Assembly in Cells. Is the F-actin severing activity of ADF important to its function in cells or is the activity too weak to be of significance? If conditions exist within cells whereby ADF can bind cooperatively to regions of F-actin, activation by increasing pH could lead to rapid fragmentation and release of ADF–actin complexes. Such conditions might occur, for example, in fibroblasts, where activation of quiescent cells with growth factors leads to restoration of motility which is accompanied by a change in cytoplasmic pH from below 7.1 to about 7.3 (Shuldiner & Rosengurt, 1982; Moolenaar et al., 1984). ADF has been observed at the leading edge of fibroblasts and in the motile growth cones of neurons (Bamburg & Bray, 1987; J. R. Jensen, M. DeWit, and J. R. Bamburg, submitted for publication). Other cells have shown cytoplasmic alkalinization of 0.1–0.2 pH unit accompanying changes in shape and secretion (Rodríguez Del Castillo et al., 1992), processes which are also accompanied by changes in the assembly state of actin filaments (Bernstein & Bamburg, 1989; Vitale et al., 1991). Much larger changes in localized pH than these average values suggest are quite possible, especially in submembrane domains underlying regions of active Na^+/H^+ exchange.

How does actin depolymerized by ADF return to the assembly competent pool? When ADF depolymerizes F-actin, the actin in the resulting complexes would contain ADP as the bound nucleotide, and the exchange of ADP for ATP is inhibited by ADF. However, another actin monomer binding protein, profilin, has the capacity to stimulate nucleotide

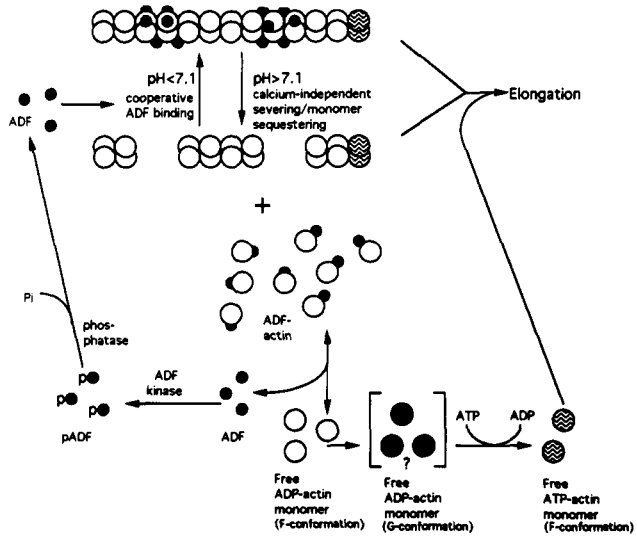

FIGURE 12: Schematic model summarizing the interactions of ADF with G- and F-actin.

exchange (Nishida, 1985; Goldschmidt-Clermont et al., 1992), even from ADF–actin complexes (S. M. Hayden and J. R. Bamburg, unpublished observations), suggesting that actin may turn over rapidly from ADF–actin complexes formed *in vivo*. Other modulators of ADF–actin binding are the tropomyosins (Bernstein & Bamburg, 1982; Bamburg & Bernstein, 1991), which inhibit ADF-induced F-actin depolymerization, and the inositol phospholipids, which have been shown to enhance the dissociation of actin from several actin binding proteins (Lassing & Lindberg, 1988; Janmay et al., 1987), including destrin (Yonezawa et al., 1990). In addition, ADF activity is regulated by phosphorylation (Morgan et al.,1993), a reaction catalyzed by cellular kinases under control of signal transduction pathways (Baorto et al., 1992). In most tissues and cells examined to date, 10–60% of the total immunoreactive ADF pool is present as an inactive, phosphorylated ADF (Morgan et al., 1993). The model presented in Figure 12 depicts the pH-dependent cooperative F-actin binding and severing/sequestering activities of ADF along with its regulation by phosphorylation. In addition, the reactivation of the actin monomer pool requiring nucleotide exchange from the ADF–actin complex is included.

Both ADF and cofilin exist in the same cells and have similar subcellular distributions within the cells (myocytes, neurons, and fibroblasts) in which they have both been examined (Bamburg & Bray, 1987; Yonezawa et al., 1987; Ono et al., 1993; J. R. Jensen, M. DeWit, and J. R. Bamburg, submitted for publication). Thus, one might ask what two functionally similar proteins are doing in the same cell. Similar questions have been raised concerning the multiple isoforms of many of the cytoskeletal proteins which come from different genes, including actin (Vandekerchove & Weber, 1978). While it seems likely that some differences in cellular function may eventually be found for ADF and cofilin, perhaps involving subtle differences in their affinities for the different actin isoforms, it is quite clear that one major reason for their existence is so that the expression of proteins with their activity can be differentially regulated in a tissue-specific fashion during development (Bamburg & Bray, 1987; Abe & Obinata, 1989; Morgan, 1990).

Since ADF, and presumably other members of its family, can provide a reactive monomer pool through which the effects of other monomer-sequestering proteins, such as profilin (Cao et al., 1992) and thymosin β_4 (Cassimeris et al., 1992; Yu et

al., 1993), can be enhanced (J. R. Bamburg, unpublished observations), the spatial and temporal regulation of ADF in cells will have a dramatic effect on the local cytoarchitecture. The fact that this protein family is so widespread in nature, including its recent discovery in plants (Kim et al., 1993), and the finding that its inactivation in yeast is a lethal mutation (Moon et al., 1993) suggest that it plays an essential and fundamental role in regulating actin filament dynamics in a wide variety of cell types.

ACKNOWLEDGMENT

We thank Alan Weeds and Mark Hawkins, Laboratory of Molecular Biology, Cambridge, for helpful discussions and for their willingness to exchange copies of manuscripts prior to submission describing our independent studies on the interactions of ADF with actin. The technical assistance of Laurie Minamide is gratefully acknowledged. We also thank Drs. Peter Gunning and Edna Hardeman of the Children's Medical Research Institute, Westmead, NSW, Australia, in whose laboratories a portion of the experiments reported here was completed during a sabbatical leave for J.R.B.

REFERENCES

Abe, H., & Obinata, T. (1989) in *Cellular and Molecular Biology of Muscle Development* (Stockdale, F., & Kedes, L., Eds.) pp 197–206, Alan R. Liss, New York.
Abe, H., Endo, T., Yamamoto, K., & Obinata, T. (1990) *Biochemistry 29*, 7420–7425.
Aboderin, A. A., Boedefeld, E., & Luisi, P. L. (1973) *Biochim. Biophys. Acta 328*, 20–30.
Adams, M. E., Minamide, L. S., Duester, G., & Bamburg, J. R. (1990) *Biochemistry 29*, 7414–7420.
Bamburg, J. R., & Bray, D. (1987) *J. Cell Biol. 105*, 2817–2825.
Bamburg, J. R., & Bernstein, B. W. (1991) in *The Neuronal Cytoskeleton* (Burgoyne, R., Ed.) pp 121–160, Wiley-Liss, New York.
Bamburg, J. R., Harris, H. E., & Weeds, A. G. (1980) *FEBS Lett. 121*, 178–182.
Bamburg, J. R., Minamide, L. S., Morgan, T. E., Hayden, S. M., Giuliano, K. A., & Koffer, A. (1991) *Methods Enzymol. 196*, 125–140.
Baorto, D. M., Mellado, W., & Shelanski, M. L. (1992) *J. Cell Biol. 117*, 357-367.
Barden, J. A., & dos Remedios, C. G. (1985) *Eur. J. Biochem. 146*, 5–8.
Berl, S., Chou, M., & Mytilineou, C. (1983) *J. Neurochem. 40*, 1397–1405.
Bernstein, B. W., & Bamburg, J. R. (1982) *Cell Motil. 2*, 1–8.
Bernstein, B. W., & Bamburg, J. R. (1989) *Neuron 3*, 257–265.
Blikstad, I., Markey, F., Carlsson, L., Persson, T., & Lindberg, U. (1978) *Cell 15*, 935–943.
Bradford, M. M. (1976) *Anal. Biochem. 72*, 248–254.
Bray, D., & Thomas, C. (1976) *J. Mol. Biol. 105*, 527–544.
Bryan, J. (1988) *J. Cell Biol. 106*, 1553–1562.
Cao, L.-G., Babcock, G. G., Rubenstein, P. A., & Wang, Y.-L. (1992) *J.Cell Biol. 117*, 1023–1029.
Carlsson, L., Nystrom, L.-E., Sundkvist, I., Markley, F., & Lindberg, U. (1977) *J. Mol. Biol. 115*, 465–483.
Cassimeris, L., Safer, D., Nachmias, V. T., & Zigmond, S. H. (1992) *J. Cell Biol. 119*, 1261–1270.
Cooke, R. (1975) *Biochemistry 14*, 3250–3256.
Cooke, R., & Murdoch, L. (1973) *Biochemistry 12*, 3927–3932.
Cooper, J. A., Walker, S. B., & Pollard, T. D. (1983) *J. Muscle Res. Cell Motil. 4*, 253–262.
Cooper, J. A., Blum, J. D., Williams, R. C. Jr., & Pollard, T. D. (1986) *J. Biol. Chem. 261*, 477–485.
Detmers, P., Weber, A., Elzinga, M., & Stephens, R. E. (1981) *J. Biol. Chem. 256*, 99–105.
Frieden, C., & Patane, K. (1985) *Biochemistry 24*, 4192–4196.
Frieden, C., & Patane, K. (1988) *Biochemistry 27*, 3812–3820.
Giuliano, K. A., Khatib, F. A., Hayden, S. M., Daoud, E. W., Adams, M. E., Amorese, D. A., Bernstein, B. W., & Bamburg, J. R. (1988) *Biochemistry 27*, 8931–8938.
Goldschmidt-Clermont, P. J., Furman, M. I., Wachsstock, D., Safer, D., Nachmias, V.T., & Pollard, T. D. (1992) *Mol. Biol. Cell 3*, 1015–1024.
Harafuji, H., & Ogawa, Y. (1980) *J. Biochem. (Tokyo) 87*, 1305–1312.
Harris, D. A., & Schwartz, J. H. (1981) *Proc. Natl. Acad. Sci. U.S.A. 78*, 6798–6802.
Harris, H. E., & Gooch, J. (1981) *FEBS Lett. 123*, 49–53.
Harris, H. E., & Weeds, A. G. (1983) *Biochemistry 22*, 2728–2741.
Harris, H. E., Bamburg, J. R., Bernstein, B. W., & Weeds, A. G. (1982) *Anal. Biochem. 119*, 102–114.
Hawkins, M., Pope, B., Maciver, S. K., & Weeds, A. G. (1993) *Biochemistry* (preceding paper in this issue).
Heacock, C. S., Brown, S. L., & Bamburg, J. R. (1982) *Natl. Cancer Inst. Monogr. No. 61*, 73–75.
Heacock, C. S., Eidsvoog, K. E., & Bamburg, J. R. (1984) *Exp. Cell Res. 153*, 402–412.
Hitchcock, S. E. (1980) *J. Biol. Chem. 255*, 5668–5673.
Houk, T. W., & Ue, K. (1974) *Anal. Biochem. 62*, 66–74.
Janmey, P. A., Iida, K., Yin, H. L., & Stossel, T. P. (1987) *J. Biol. Chem. 262*, 12228–12236.
Kim, S.-R., Kim, Y., & An, G. (1993) *Plant Mol. Biol. 21*, 39–45.
Koffer, A., Edgar, A. J., & Bamburg, J. R. (1988) *J. Muscle Res. Cell Motil. 9*, 320–328.
Kouyama, T., & Mihashi, T. (1981) *Eur. J. Biochem. 114*, 33–38.
Laemmli, U. K. (1970) *Nature 227*, 680–684.
Lal, A. A., Brenner, S. L., & Korn, E. D. (1984) *J. Biol. Chem. 259*, 13061–13065.
Lassing, I., & Lindberg, U. (1988) *J. Cell. Biochem. 37*, 255–267.
Lees, A., Haddad, J. G., & Lin, S. (1984) *Biochemistry 23*, 3038–3047.
Mabuchi, I. (1983) *J. Cell Biol. 97*, 1612–1621.
Maekawa, S., Nishida, E., Ohta, Y., & Sakai, H. (1984) *J. Biochem. (Tokyo) 95*, 377–385.
Mannherz, H. G., Goody, R. S., Konrad, M., & Nowak, E. (1980) *Eur. J. Biochem. 104*, 367–379.
Martin, J. B., & Doty, D. M. (1949) *Anal. Chem. 21*, 965–967.
Matsudaira, P. T., & Burgess, D. R. (1978) *Anal. Biochem. 87*, 386–396.
Matsuzaki, F., Matsumoto, S., Yahara, I., Yonezawa, N., Nishida, E., & Sakai, H. (1988) *J. Biol. Chem. 263*, 11564–11568.
Miki, M. (1991) *Biochemistry 30*, 10878–10884.
Miki, M., Ohnuma, H., & Mihashi, K. (1974) *FEBS Lett. 46*, 5359–5362.
Minamide, L. S., & Bamburg, J. R. (1990) *Anal. Biochem. 190*, 66–70.
Mockrin, S. C., & Korn, E. D. (1980) *Biochemistry 19*, 5359–5362.
Moolenaar, W. H., Tertoolen, L. G. J., & deLaat, S. W. (1984) *J. Biol. Chem. 259*, 7563–7570.
Moon, A. L., Janmey, P. A., Louie, K. A., & Drubin, D. G. (1993) *J. Cell Biol. 120*, 421–435.
Morgan, T. E. (1990) Ph.D. Thesis, Colorado State University, Fort Collins, CO.
Morgan, T. E., Lockerbie, R. O., Minamide, L. S., Browning, M. D., & Bamburg, J.R. (1993) *J. Cell Biol. 122*, 623–633.
Moriyama, K., Nishida, E., Yonezawa, N., Sakai, H., Matsumoto, S., Iida, K., & Yahara, I. (1990) *J. Biol. Chem. 265*, 5768–5773.
Moriyama, K., Yonezawa, N., Sakai, H., Yahara, I., & Nishida, E. (1992) *J. Biol. Chem. 267*, 7240–7244.
Murphy, D. B., Gray, R.O., Grasser, W. A., & Pollard, T. D. (1988) *J. Cell Biol. 106*, 1947–1954.
Nishida, E. (1985) *Biochemistry 24*, 1160–1164.

Nishida, E., Maekawa, S., Muneyuki, E., & Sakai, H. (1984) *J. Biochem. (Tokyo) 95*, 387–398.
Nishida, E., Muneyuki, E., Maekawa, S., Ohta, Y., & Sakai, H. (1985) *Biochemistry 24*, 6624–6630.
Nowak, E., Strzelecka-Golaszewska, H., & Goody, R. S. (1988) *Biochemistry 27*, 1785–1792.
Ono, S., Abe, H., Nagacka, R., & Obinata, T. (1993) *J. Muscle Res. Cell Motil. 14*, 195–204.
Pardee, J. D., & Spudich, J. A. (1982) *Methods Cell Biol. 24*, 271–289.
Pollard, T. D., & Weeds, A. G. (1984) *FEBS Lett. 170*, 94–98.
Pollard, T. D., & Cooper, J. A. (1986) *Annu. Rev. Biochem. 55*, 987–1035.
Quirk, S., Maciver, S. K., Ampe, C., Doberstein, S. K., Kaiser, D. A., VanDamme, J., Vandekerckhove, J. S., & Pollard, T. D. (1993) *Biochemistry* (in press).
Rodríguez Del Castillo, A., Vitale, M. L., & Trifaró, J.-M. (1992) *J. Cell Biol. 119*, 797–810.
Schuldiner, S., & Rozengurt, E. (1982) *Proc. Natl. Acad. Sci. U.S.A. 79*, 7778–7782.
Takagi, T., Konishi, K., & Mabuchi, I. (1988) *J. Biol. Chem. 263*, 3097–3102.
Tanaka, M., & Shibata, H. (1985) *Eur. J. Biochem. 151*, 291–297.
Tobacman, L. S., & Korn, E. D. (1982) *J. Biol. Chem. 257*, 4166–4170.
Vandekerckhove, J., & Weber, K. (1978) *Eur. J. Biochem. 90*, 451–462.
Vitale, M. L., Rodríguez Del Castillo, A., Tchakarov, L., & Trifaró, J.-M. (1991) *J. Cell Biol. 113*, 1057–1067.
Wagner, M., & Wegner, A. (1985) *Biochemistry 24*, 1035–1040.
Yonezawa, N., Nishida, E., & Sakai, H. (1985) *J. Biol. Chem. 260*, 14410–14412.
Yonezawa, N., Nishida, E., Koyasu, S., Maekawa, S., Ohta, Y., Yahara, I., & Sakai, H. (1987) *Cell Struct. Funct. 12*, 443–452.
Yonezawa, N., Nishida, E., Iida, K., Yahara, I., & Sakai, H. (1990) *J. Biol. Chem. 265*, 8382–8386.
Yu, F.-X., Lin, S.-C., Morrison-Bogorad, M., Atkinson, M. A. L., & Yin, H. L. (1993) *J. Biol. Chem. 268*, 502–509.